Journal of Sound and Vibration (1998) **218**(4), 697–709
Article No. sv981839

SONIC STOP-BANDS FOR PERIODIC ARRAYS OF METALLIC RODS: HONEYCOMB STRUCTURE

M. S. KUSHWAHA† AND B. DJAFARI-ROUHANI

Laboratoire de Dynamique et Structures des Matériaux Moléculaires, U.R.A.C.N.R.S. No. 801, *U.F.R. de Physique*, *Université de Lille I*, *F59655 Villeneuve d'Ascq Cedex*, *France*

(*Received* 6 *March* 1998, *and in final form* 1 *July* 1998)

Extensive band structures have been computed for periodic arrays (in the honeycomb structure) of rigid metallic rods in air. Multiple complete acoustic stop bands have been obtained within which sound and vibrations are forbidden. These gaps start opening up for a filling fraction $f \geqslant 8\%$ and tend to increase with the filling fraction, exhibiting a maximum at the close-packing. A tandem structure has also been proposed that allows an ultrawideband filter for environmental or industrial noise to be achieved in the desired frequency range. This work is motivated by the recent experimental observation of sound attenuation on the sculpture by Eusebio Sempere, exhibited at the Juan March Foundation in Madrid [21] and complements the corresponding theoretical work [22, 23].

1. INTRODUCTION

Once in a while a topic emerges that has a universal appeal. Such is the case with periodic dielectric structures becoming known as photonic crystals [1, 2]. Photonic crystals can be used to manipulate the path of light, and promise to be as important to the design of optical devices as semiconductors were to the development of electronic devices. The exotic properties (and their consequences) of these materials are thought to arise from multiple reflections at the periodically distributed scatterers, which add up to prevent light from propagating over a wide range of frequencies. Within such a forbidden band of frequencies (also called band gaps or stop bands), optical modes, spontaneous emission, and zero-point fluctuations are all absent. Because of its promixed ability to influence spontaneous emission and to pave the way to light localization [3], the pursuit of photonic band gaps has been the major motivation for studying photonic crystals. Photonic crystals consist of periodically modulated dielectric materials with periodicity on the scale of the wavelength of light. This constitutes an important

† Permanent address: Institute of Physics, University of Puebla, P.O. Box J-48, Puebla 72570, Mexico.

0022–460X/98/490697 + 13 $30.00/0

regime of mesoscopic physics with exciting new technological applications, which is just beginning to be explored.

Analogies between subfields of physics have almost always opened amazingly fruitful avenues in research. An exciting example is the recent upsurge in the growing interest in analogous investigations on phononic crystals [4–16]. These are two- and three-dimensional periodic elastic/acoustic composites which can exhibit complete acoustic stop bands. The term *complete* refers to the gap which exists independent of the polarization of the wave and its direction of propagation. In analogy to the photonic crystals, the prime interest of the band theorists was focused on the existence of spectral gaps in periodic systems and mobility gaps in disordered systems. Within a complete acoustic band gap, sound, vibrations, and phonons are all absent. This is of interest for applications such as acoustic filters, improvement in the design of transducers, and noise control [3]; as well as for pure physics concerned with the Anderson localization of sound and vibrations [17, 18]. Piezoelectric, pyroelectric, and piezomagnetic composites are already known to have long standing applications as medical ultrasonics and naval transducers, as well as for related tasks in medical imaging [19, 20]. Such composites were initially fabricated for sonar applications and are now widely used for ultrasonic transducers.

It is interesting to remark that in all *artificial* periodic structures—dielectric composites, elastic composites, magnetic composites, etc.—the existence of *complete* gaps is attributed to the joint effect of the Bragg diffraction and the Mie scattering. The destructive interference due to Bragg diffraction accompanied by the Mie resonances due to strong scattering from individual scatterer is the conceptual base of the complete gaps. The latter becomes effective when the dimension of the scatterers is close to an integer multiple of wavelength [3].

In the quest for achieving complete gaps one must resort to the band structure calculations. These have been performed for several geometries of periodic elastic composites and for various types of waves [4–16]. One-dimensional (1D) periodic systems (superlattices, for example) allow longitudinal, transverse, and mixed modes. Two-dimensional (2D) composites permit the propagation of pure transverse and mixed modes independently; no longitudinal modes are possible, however. In three-dimensional (3D) composites the longitudinal and transverse modes are strongly coupled, thus complicating the nature of the eigenmodes and the corresponding computation. A drastic simplification arises in the case of liquids and gases, which support only dilatational (acoustic) waves. In what follows we will be concerned with such a single polarization of dilatational waves.

The present work is motivated by the recent experimental measurements of sound attenuation on the sculpture, by Eusebio Sempere, exhibited at the Juan March Foundation in Madrid [21]. It consists of a periodic distribution of hollow stainless steel cylinders, with diameter of 2·9 cm and a unit cell of edge 10 cm. The cylinders are fixed on a circular platform (4 m in diameter) which can rotate on a vertical axis. The sound attenuation was measured in the outdoor conditions for the wave-vectors perpendicular to the cylinders' vertical axis. The sculpture thus corresponds to a cermet topology with a volume fraction occupied by the scatterers of 0·066 and a sound-speed ratio of 17·9. The experimentalists' speculation, based on their observation, was that the sound attenuation peak at 1·67 kHz could be ascribed to the formation of the first (i.e., the lowest) gap in this sculpture. We call attention to the two important points: first, the sculpture represents a 2D periodicity in the x–y plane (provided the cylinders' vertical axis is presumed to be along the z-axis); second, the sculpture consists of finite (in length) cylinders and is not strictly periodic (in the sense that it does not extend infinitely in the x–y plane).

This experimental finding was soon followed by a rigorous theoretical investigation enmbarking on the *ideal* situation and employing the actual experimental parameters (we refer to the true dimensions of the sculpture) [22–24]. The complete band structure and density of states (DOS) were computed for an ideal 2D periodic system to draw the following conclusions. It was found that for the experimental situation (i.e., for the cylinders 2·9 cm in diameter and system-period of 10 cm implying to the filling fraction $f = 0{\cdot}066$) there is *no* acoustic gap for frequencies below 6·4 kHz. However, the DOS reveal prominent minima at 1·7 and 2·4 kHz. These frequencies do agree with those of the first two attenuation maxima in reference [21], and are indeed related to the diffraction from [100] and [110] planes (i.e., the $\bar{X}$ and $\bar{M}$ high symmetry points in the Brillouin zone). Thus, *even with idealization*, Sempere's sculpture was seen to exhibit only pseudogaps—*not full gaps*. We refer the readers to references [23, 24] for other details regarding the circumstances where such a sculpture could exhibit complete gaps. It is noteworthy that the term complete was reserved in the sense that both experiment and theory ignored the possibility of filtration of sound along the vertical axis of the cylinders.

In this work, a 2D honeycomb (or hexagonal) structure consisting of rigid metallic (for example, stainless steel) rods, in a rarer medium (for example, air)—analogous to Eusebio Sempere's sculpture is considered. In a sense, this complements the previous work on 2D periodic systems in references [22, 23] to investigate whether or not there could exist a *complete* gap in the 2D systems with a honeycomb structure. It has been found that the honeycomb structure can give rise to genuine multiple stop bands, whose frequency range can be raised (lowered) by decreasing (increasing) the period of the system. The details of the theory of band structure for elastic/acoustic composites of arbitrary periodicity and inhomogeneity can be found in reference [8]. However, the methodological details needed to accomplish the problem at hand are described succinctly in the following section.

2. FORMALISM

A 2D periodic system made up of *infinitely* rigid metallic rods in air—with honeycomb structure—is considered. The assumption of infinite rigidity means the modulus of compressibility of the inclusions is infinite. However, in order to keep the usual speed of sound, it is assumed that the density of the inclusions is also infinite. This hypothesis, which is very well justified for the metallic (for example, stainless steel) inclusions in air, then implies that the sound does not penetrate such inclusions and hence the propagation is confined and predominant only in the air. In other words there is no communication between the air inside and outside. Then it really also does not matter whether these inclusions are hollow or solid within.† Therefore, the calculation at hand simplifies considerably because the transverse speed of sound c_t is zero in gases (and liquids). Nevertheless, the ordinary wave equation is inapplicable to the inhomogeneous media. The correct wave equation—simply the equation of motion in the absence of an external force—is

$$\rho \frac{\partial^2 \mathbf{u}}{\partial t^2} = \mathbf{\nabla}(\rho c_l^2 \mathbf{\nabla} \cdot \mathbf{u}), \tag{1}$$

where $\rho(\mathbf{r})$ is the mass density and $\mathbf{c}_l(\mathbf{r})$ is the longitudinal speed of sound. Only if ρc_l^2 is independent of the position, do all the three components of $\mathbf{u}(\mathbf{r}, t)$ satisfy the ordinary wave equation. In the general case, one observes, from equation (1), that $\mathbf{\nabla} \times (\rho \mathbf{u}) = 0$. Hence, it is possible to define a scalar potential $\Phi(\mathbf{r}, t)$ such that $\rho \mathbf{u} = \mathbf{\nabla}\Phi$. Then equation (1) may be cast in the form

$$(C_{11})^{-1} \frac{\partial^2 \Phi}{\partial t^2} = \mathbf{\nabla} \cdot (\rho^{-1} \mathbf{\nabla} \Phi), \tag{2}$$

where $C_{11} = \rho c_l^2$ is the longitudinal elastic constant. Taking advantage of the 2D periodicity, the quantities $\rho^{-1}(\mathbf{r})$ and $C_{11}^{-1}(\mathbf{r})$ in the Fourier series are expanded

$$\rho^{-1}(\mathbf{r}) = \sum_{\mathbf{G}} \sigma(\mathbf{G})\, \mathrm{e}^{\mathrm{i}\mathbf{G}\cdot\mathbf{r}}, \qquad C_{11}^{-1}(\mathbf{r}) = \sum_{\mathbf{G}} \zeta(\mathbf{G})\, \mathrm{e}^{\mathrm{i}\mathbf{G}\cdot\mathbf{r}}, \tag{3}$$

where $\mathbf{G}$ and $\mathbf{r}$ are the 2D reciprocal and direct lattice vectors. The solution of equation (2) is given by means of the Bloch theorem:

$$\Phi(\mathbf{r}, t) = \mathrm{e}^{\mathrm{i}(\mathbf{K}\cdot\mathbf{r} - \omega t)} \sum_{\mathbf{G}} \Phi_{\mathbf{K}}(\mathbf{G})\, \mathrm{e}^{\mathrm{i}\mathbf{G}\cdot\mathbf{r}}. \tag{4}$$

Here $\mathbf{K}$ is a 2D Bloch vector. With the aid of equations (3) and (4), equation (2) yields an infinite set of equations for eigenvalues $\omega(\mathbf{K})$ and eigenvectors $\Phi_{\mathbf{K}}(\mathbf{G})$:

$$\sum_{\mathbf{G}'} [\sigma(\mathbf{G} - \mathbf{G}')(\mathbf{K} + \mathbf{G}) \cdot (\mathbf{K} + \mathbf{G}') - \zeta(\mathbf{G} - \mathbf{G}')\omega^2] \Phi_{\mathbf{K}}(\mathbf{G}') = 0. \tag{5}$$

This equation is applied to a 2D periodic system of circular inclusions (medium i) in a background (medium b); the filling fraction of the metallic rods is f. The

† The authors thank one of the referees who warned that the assumption of infinite rigidity may break down if tried to approximate an array of hollow tubes having an in-band resonance. He suggests that there the large monopole amplitudes could filter to the exterior tube walls and hence alter the acoustic field substantially.

corresponding densities (elastic constants) are ρ_i, $\rho_b(C_{11i}, C_{11b})$. Then it is a simple matter to show that [8]

$$\sigma(\mathbf{G}) = \begin{cases} \rho_i^{-1} f + \rho_b^{-1}(1-f) \equiv \overline{\rho^{-1}}, & \text{for} \quad \mathbf{G} = 0, \\ (\rho_i^{-1} - \rho_b^{-1})F(\mathbf{G}) \equiv \Delta(\rho^{-1})F(\mathbf{G}), & \text{for} \quad \mathbf{G} \neq 0, \end{cases} \tag{6}$$

where the structure factor $F(\mathbf{G})$ is given by

$$F(\mathbf{G}) = \frac{1}{A_c} \int_i \mathrm{d}^2 r \, \mathrm{e}^{-\mathrm{i}\mathbf{G}\cdot\mathbf{r}} = 2fJ_1(Gr_0)/(Gr_0), \tag{7}$$

where $J_1(x)$ is the Bessel function of the first kind of order one, A_c is the area of the unit cell, the integration is limited to a cylinder of radius r_0, and the filling fraction

$$f = \pi r_0^2 / A_c = \frac{2\pi}{\sqrt{3}} (r_0/a)^2, \tag{8}$$

where a is the period (or lattice constant) of the system. An equation analogous to equation (6) can be written for $\zeta(\mathbf{G})$ in terms of C_{11}^{-1}. Then equation (5) can be cast in the form

$$\sum_{\mathbf{G}' \neq \mathbf{G}} F(\mathbf{G} - \mathbf{G}')[\Delta(\rho^{-1})(\mathbf{K} + \mathbf{G}) \cdot (\mathbf{K} + \mathbf{G}') - \Delta(C_{11}^{-1})\omega^2]\Phi_{\mathbf{K}}(\mathbf{G}')$$
$$+ [\overline{\rho^{-1}}|\mathbf{K} + \mathbf{G}|^2 - \overline{C_{11}^{-1}}\omega^2]\Phi_{\mathbf{K}}(\mathbf{G}) = 0. \tag{9}$$

Interestingly, this eigenvalue equation for dilatational modes is formally the same as the eigenvalue equation for *transverse* modes in the corresponding solid composites with 2D periodicity (see, for example, equation (6) in reference [6]). It is not difficult to rewrite equation (9) in the form of a standard eigenvalue problem [8], which is in fact performed at the computational level. Doing so ensures a drastic saving in computational time.

For the purpose of computation, the number of plane waves was limited to 169. This resulted in reliably very good convergence; at least up to the lowest 20th bands. By increasing the number of plane waves to 441, our results change, after the 20th band, by less than 1%. This emboldens our confidence in the adequacy of our results based on the 169 plane waves, particularly in the low-frequency regime where the *complete* stop bands were found.

Note that our numerical results, presented in the following section, correspond specifically to the composite system made up of stainless steel inclusions in air. However, the results remain quite unaltered as long as the assumption of infinite rigidity prevails (see above). This is clearly an artifact of the huge contrast in the material parameters of the inclusions and the background.

3. RESULTS AND DISCUSSION

Figure 1 depicts the first Brillouin zone for the honeycomb (hexagonal) structure which is of immediate concern for the work reported in this paper.

Figure 2 illustrates the band structure and the density of states (DOS) for rigid rods in the hexagonal structure; for a filling fraction of $f = 0{\cdot}55$. The lowest *ten* bands are shown. The plots are rendered in terms of the eigenfrequency $v = \Omega(\bar{c}_l/a)$ [where a is the lattice constant, Ω is the dimensionless frequency, and $\bar{c}_l = \sqrt{(\rho^{-1}/C_{11}^{-1})}$] versus the dimensionless Bloch vector $\mathbf{k} = \mathbf{K}a/2\pi$. The left part of the triptych represents the band structure in the three principal symmetry directions, letting $\mathbf{k}$ scan only the periphery of the irreducible part of the first Brillouin zone (see shaded region in Figure 1). The middle part is the result of an extensive scanning of $|\mathbf{k}|$ in the irreducible part of the Brillouin zone—the interior of this zone and its surface, as well as the principal directions shown in the left part of the figure. Each curve here corresponds to some direction of $\mathbf{k}$. The DOS in the right part of the triptych has been calculated on the basis of the scanning in the middle part, which corresponds to 1326 $\mathbf{k}$-points within the irreducible part of the first Brillouin zone. The three parts of the triptych in Figure 2 together demonstrate that there are, indeed, four genuine complete gaps (the shaded regions) and such calculations are considered as essential. It should be pointed out that the third band is almost a flat line (with vanishing group velocity) and thus remains indiscernible from the upper edge of the first hatched region. This remark should avoid any confusion the reader may have about the spatial positions of the gaps as explained next. Out of these the first gap is defined by the maximum (minimum) of the second (third) band at $\Gamma(J)$ point, the second one by the maximum (minimum) of the sixth (seventh) bands at $J(\Gamma)$ point, the third one by the maximum (minimum) of the seventh (eighth) bands at J point, and the fourth one by the maximum (minimum) of the ninth (tenth) bands at Γ point. As such,

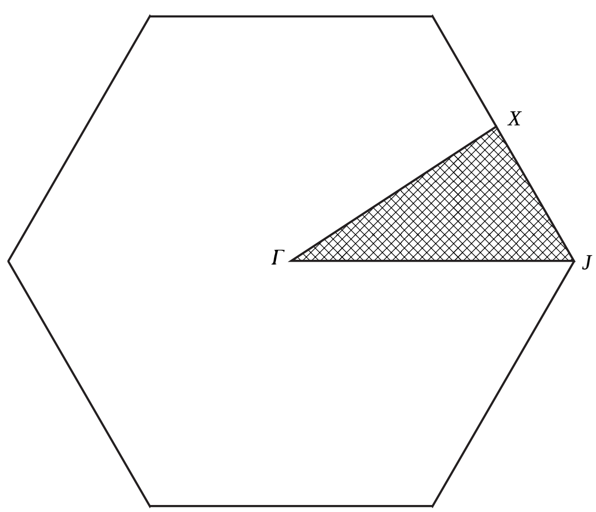

Figure 1. The first Brillouin zone of the honeycomb structure showing the symmetry points and axes.

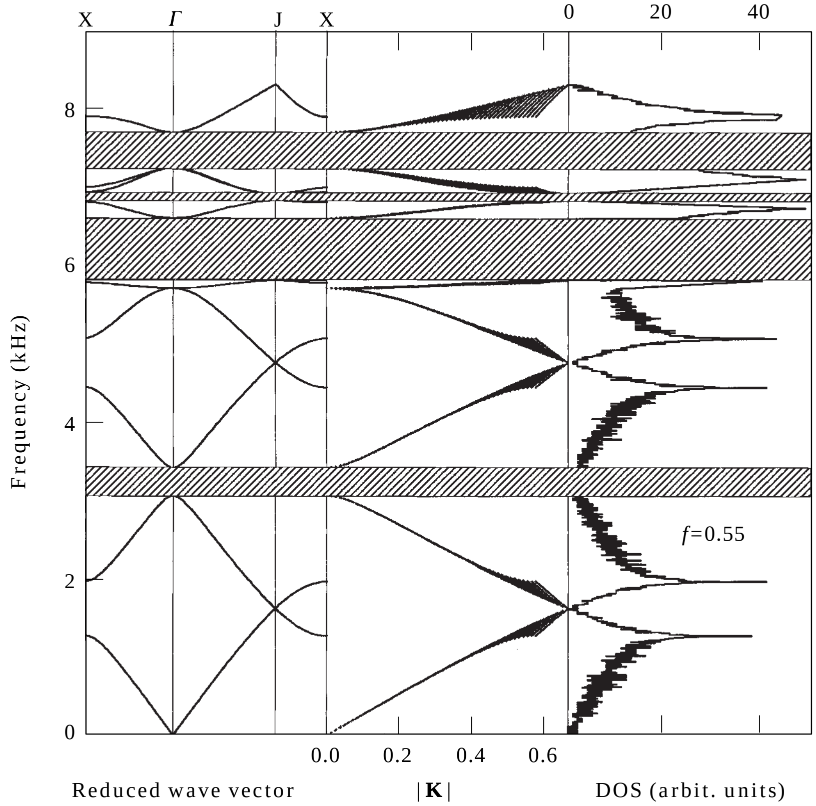

Figure 2. Acoustic band structure and density of states for a 2D array of *rigid* metallic rods in air. The plots are rendered in terms of the frequency $\nu = \Omega(\bar{c}_l/a)$ [where a is the lattice constant, Ω is the dimensionless frequency, and $\bar{c}_l = \sqrt{(\rho^{-1}/C_{11}^{-1})}$] versus dimensionless Bloch vector $\mathbf{k} = \mathbf{K}\, a/2\pi$. The filling fraction is $f = 0{\cdot}55$ and the period is $a = 10$ cm. The triptych is comprised of three parts. In the left panel, the band structure is plotted in the three principal symmetry directions, letting the Bloch vector $\mathbf{k}$ scan only the periphery of the irreducible part of the first Brillouin zone. The middle panel demonstrates a novel way of plotting the eigenvalues as a function of $|\mathbf{k}|$; i.e., the distance of a point in the irreducible part of the Brillouin zone from the Γ point. The right panel illustrates the DOS. Attention is drawn to the *four* complete stop-bands (hatched region) extending throughout the Brillouin zone. Note that the third band is almost a flat line and remains indiscernible from the upper edge of the first hatched region that refers to the first gap.

the first and second (third and fourth) gaps are indirect (direct) ones in the language of solid state physics.

Next we plot the gap-widths of the four existing stop bands within the first ten bands in the honeycomb structure in Figure 3. The size of a complete gap is usually expressed as the ratio of the gap-width and the midgap frequency. The gap-width on the y-axis represents just a difference in frequencies of the top and bottom of the stop bands, for a given filling fraction. As seen from the figure, the filling fraction must exceed a certain minimum value, f_{min}, for a gap to be opened. This leads us to infer that there is no band gap for $f_{min} \leqslant 0{\cdot}08$. Except for the third gap which opens in a very narrow range of filling fraction ($0{\cdot}53 \leqslant f \leqslant 0{\cdot}56$), the rest of the three gaps observe a maximum and a minimum before the close-packing (i.e., when the cylinders start touching each other). It is interesting to note that at $f = 40\%$ there are no gaps opening up in the system, just as for $f \leqslant 8\%$. All the three gaps, which open over a wide range of filling fraction, observe a second maximum at the close-packing where the band structure reveals flat, degenerate bands depicting huge stop bands. This is quite easy to understand. In the limit of close-packing, the resultant 2D periodic system allows almost exactly isolated vortices and hence the sound cannot spin around the rigid cylinders.

Finally, the fabrication of a multiperiodic system in tandem that could be designed so as to give rise to wider stop bands in the *desired* frequency range is proposed. The band-gap edges of the lowest stop band are computed as a function of the filling fraction for a large number of systems with different periods (the lattice constants). The numerical results of such investigations are illustrated in Figure 4. The "wedges", labelled 1 to 9, correspond to different periods (in the increasing order from top to bottom) and are based on the numerous band structure calculations—one for every value of the filling fraction f. These are really eigenvalue problems for the reduced frequency Ω as a function of the Bloch vector $\mathbf{k}$ scanned in all directions. It is important to note here (and, in fact, throughout this paper) that the eigenfrequency ν is inversely proportional to the period of the system. That means that, given the specific medium in the background, the

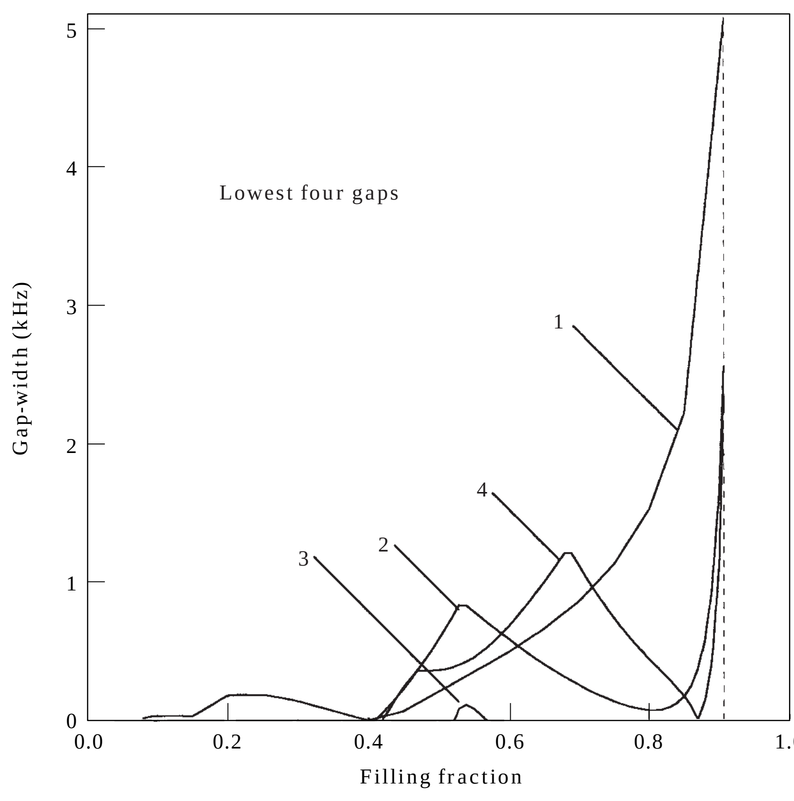

Figure 3. Gap-widths of the existing four stop-bands versus filling fraction for a 2D array of *rigid* metallic rods in air. The period of the system (i.e., the lattic constant) $a = 10$ cm. The vertical dotted line refers to the close-packing value ($f = 0{\cdot}9068$). Evident is the fact that there is no acoustic stop-band for $f \leqslant 8\%$. The numbers 1 to 4 refer to the lowest, second lowest, third lowest and the uppermost (fourth) gaps in Figure 1.

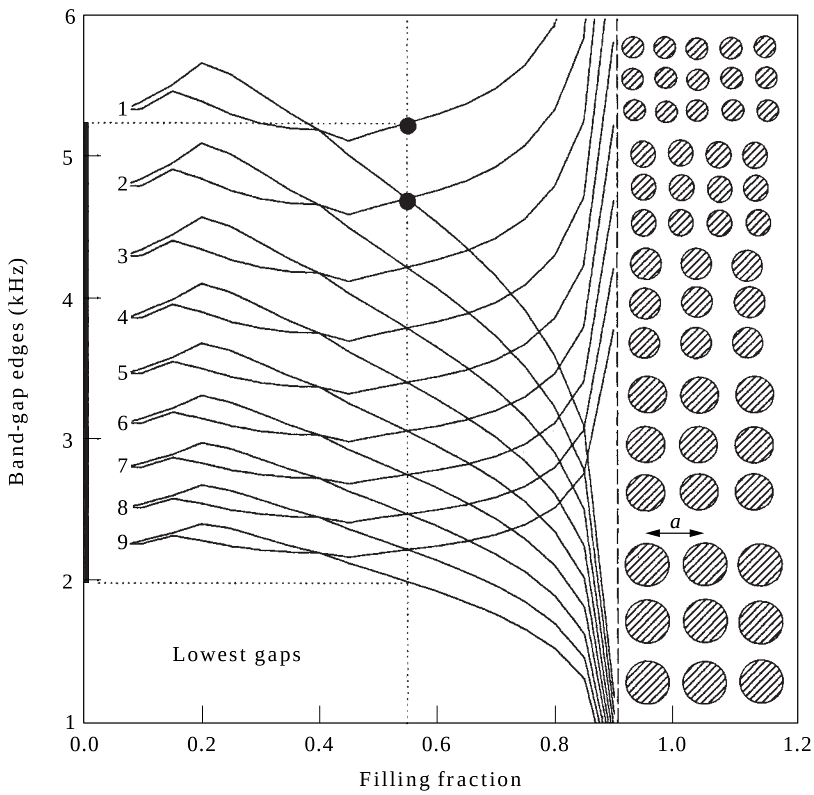

Figure 4. Design of an ultra-wide-band filter corresponding to the lowest stop band in Figure 1. Inset: schematic of the cross-section of tandem structure of (periodic) 2D arrays of *rigid* metallic rods in the honeycomb structure—what is shown is the front of a face of a unit cell of an individual periodic system. The "wedges" numbered 1–9 correspond, respectively, to the periods of 6·51, 7·24, 8·06, 8·98, 10·0, 11·13, 12·39, 13·80 and 15·37 cms. Each of the nine sets produces a stop band, whose upper and lower edges are plotted as a function of the filling fraction *f*. For $f = 0{\cdot}55$ (vertical ···· line), the nine stop bands join precisely so as to form a "super stop band" within a frequency range between 1·99 and 5·23 kHz (see the bold vertical frequency bar between the two horizontal dotted lines). The vertical – – – line refers to the close-packing value $f = 0{\cdot}9068$. This is the most convenient way of demonstrating the existence of stop-bands in a given periodic system.

frequencies of a "wedge" for a period of 1 cm will be 10 times higher than those of a "wedge" corresponding to a period of 10 cm. Consider two dots on "wedge" no. 1 for a filling fraction $f = 0{\cdot}55$. The dots mark the upper and lower edges of the stop band in the band structure and the vertical distance between them is the width of the stop band. Now the ratio of the two frequencies (specified by the dots) is calculated and the next "wedge" no. 2 is created such that its upper edge (at the same *f*) crosses the lower edge of "wedge" no. 1. The same procedure is repeated for all the nine "wedges" depicted in Figure 4. In fact, we start with "wedge" no. 5 that corresponds to a period of $a = 10$ cm. The optimum situation is embarked on, which refers to the lesser possible number of periodic composites and the smaller possible filling fraction—the former point concerns the cost and the latter hints to eventually avoiding construction of a wall of rigid cylinders. The filling fraction $f = 55\%$ is appealed to, where only nine 2D periodic composites in honeycomb structure are enough to guarantee a "super stop band" from 1·99

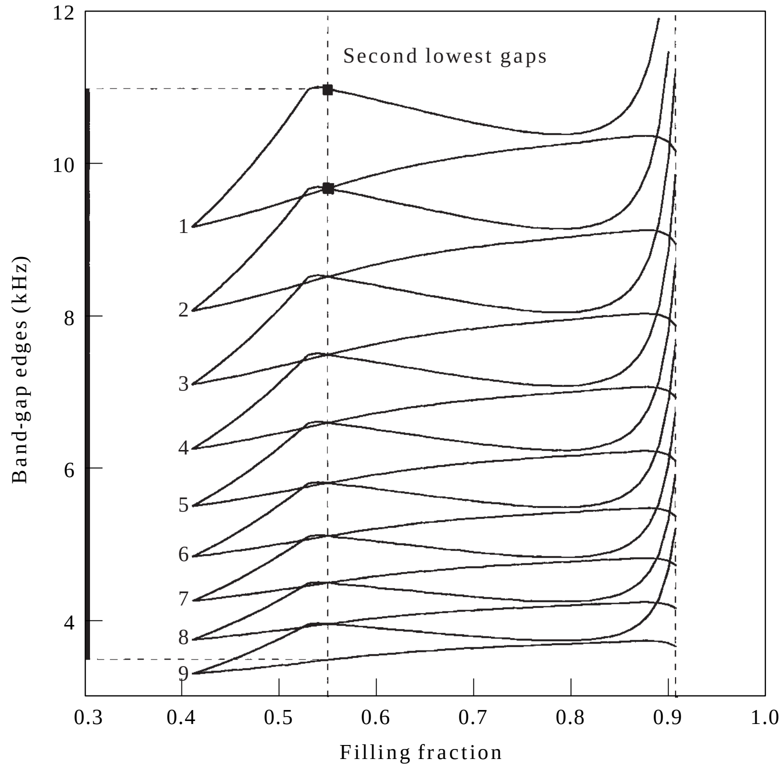

Figure 5. The same as in Figure 4, but corresponding to the second lowest stop band in Figure 1. The "wedges" numbered 1–9 correspond, respectively, to the periods of 6·00, 6·82, 7·74, 8·80, 10·00, 11·36, 12·90, 14·66 and 16·65 cm. For $f = 0{\cdot}55$ (the vertical dashed line), the nine stop bands join precisely so as to form a "super stop band" within a frequency range between 3·48 and 11·00 kHz (see the bold vertical frequency bar between the two horizontal dotted lines).

to 5·23 kHz. The range of the "super stop band" is highlighted by a bold vertical frequency bar in Figure 4. Within the "super stop band" the multiperiodic system (designed in tandem) stands still and total silence reigns. By this we mean that if one tries to transmit a wide-band wave through the tandem structure one will achieve a zero transmission within the range of the "super stop band". The completeness of such a "super stop band" is promised due to the overlapping of the individual stop bands in the neighboring composites. However, the frequency range of such a "super stop band", as mentioned above, is at the will of the designer—by increasing (decreasing) the period of the composites one can lower (raise) the frequency range of the stop bands and hence of the "super stop bands".

Note that the second lowest stop band in Figure 1 is the largest one in the range of filling fraction defined by $0{\cdot}45 \leqslant f \leqslant 0{\cdot}60$. Figure 5 illustrates the design of an ultra-wide-band filter corresponding to the second lowest stop band in Figure 1. The scheme of designing such a filter is the same as outlined in the preceding paragraph. We focus at the same filling fraction ($f = 0{\cdot}55$). As it is evident, the tandem structure in this case gives rise to a "super stop band" that ranges from 3·48 to 11·00 kHz. The rest of the discussion related to Figure 4 is still valid.

4. SUMMARY

To conclude, using simple mathematical tools employing the theory of elasticity, it is demonstrated that the 2D periodic system of rigid metallic rods in the honeycomb structure can give rise to complete stop bands. It is observed that a minimal filling fraction $f \approx 8\%$ is needed for the obtention of the lowest forbidden frequency band. The 2D tandem structures proposed here could be designed to achieve large "super stop bands" within the desired frequency range. The frequency range of such "super stop bands" can be raised (lowered) by decreasing (increasing) the period (or lattice constant) of the constituent systems. In analogy to the photonic and phononic cases, within the frequency range of stop bands sound and vibrations would be forbidden. Thus, a small vibrator (or defect) introduced into an otherwise periodic system would remain unable to generate sound within the gaps. The weakly disordered system should, on the contrary, exhibit localized modes within the gaps. The existence of complete stop bands is thus closely associated with the Anderson localization of sound and vibrations.

It is noteworthy that the existence of a complete gap in these "phononic crystals" guarantees the perfect reflection (and hence no transmission) of the excited acoustic wave within the frequency range of the stop band. But this does not mean that the intensity of the backscattered part of the incoming wave vanishes. The technological interest behind fabricating such "phononic crystals" is to enable the medium to prohibit the incoming wave within a desired (or tailor-made) forbidden frequency range. Consequently, such periodic composites that exhibit complete stop bands can behave as acoustic filters that prohibit sound propagation at certain frequencies while allowing practically free (provided that the absorption is scaled down to a minimum) propagation at others.

Comparing the present results with those on the 2D square lattice systems [21], it is found the magnitudes of the gaps are larger and the range of the filling fractions over which such gaps exist are wider in the honeycomb structure rather than in the square lattice. This is a reasonable result, because the constant energy surfaces in the hexagonal lattice are closer to a circular shape than those of a square lattice. A similar conclusion has been drawn in the case of single-polarized sound waves (transverse modes) in the 2D periodic systems of solid composites [9].

Figures 4 and 5 address indirectly a typical question concerned with the strategy of unwanted noise abatement: is it feasible to devise low-tech means that can forbid the sound propagation in the human audible range of frequencies (20 Hz–20 kHz)? This is a very important question that has become a major concern of scientists, engineers, and architects involved in the design of the buildings and in the planning of the cities, working together to find technically feasible solutions to the problem of noise. Fundamental to bring about a solution is the better understanding of sound propagation through the city streets and in the atmosphere above the city. For such an understanding the availability of band structures is essential. This letter is simply meant to emphasize the fundamental issues involved in the sister subject of band-gap engineering of periodic composite systems. Our theoretical results suggest a feasible designing of an ultrawideband filter for environmental or industrial noise in air (or water) according to the required specifications.

ACKNOWLEDGMENTS

One of us (M.S.K.) gratefully acknowledges the hospitality of the Laboratoire de Dynamique et Structure des Matériaux Moléculaires, U.R.A.C.N.R.S. No. 801, University of Lille I. He would also like to express his sincere thanks to the "Ministére de l'Education, de la Recherche et de la Technologie" and to the "Conseil Régional Nord-Pas de Calais" for the financial support. This work was partially supported by CONACYT, Mexico, Grant No. 2373-PE.

REFERENCES

1. E. Yablonovitch 1987 *Physical Review Letters* **58**, 2059–2062. Inhibited spontaneous emission in solid state physics and electronics.
2. S. John 1987 *Physical Review Letters* **58**, 2486–2489. Strong localization of photons in certain disordered dielectric superlattices.
3. For a recent extensive review, see M. S. Kushwaha 1996 *International Journal of Modern Physics* **B10**, 977–1094. Classical band structure of periodic elastic composites.
4. A. A. Ruffa 1992 *Journal of Acoustical Society of America* **91**, 1–11. Acoustic wave propagation through periodic bubbly liquids.
5. M. M. Sigalas and E. N. Economou 1992 *Journal of Sound and Vibrations* **158**, 377–382. Elastic and acoustic wave band structure.
6. M. S. Kushwaha, P. Halevi, L. Dobrzynski and B. Djafari-Rouhani 1993 *Physical Review Letters* **71**, 2022–2025. Acoutsic band structure of periodic elastic composites.
7. M. Sigalas and E. N. Economou 1993 *Solid State Communication* **86**, 141–143. Band structure of elastic waves in two dimensional systems.
8. M. S. Kushwaha, P. Halevi, G. Martinez, L. Dobrzynski and B. Djafari-Rouhani 1994 *Physical Review* **B49**, 2313–2322. Theory of acoustic band structure of periodic elastic composites.
9. M. S. Kushwaha and P. Halevi 1994 *Applied Physics Letters* **64**, 1085–1087. Band-gap engineering in periodic elastic composites.
10. J. O. Vasseur, B. Djafari-Rouhani, L. Dobrzynski, M. S. Kushwaha and P. Halevi 1994 *Journal of Physics*: *Condensed Matter* **6**, 8759–8770. Complete acoustic band gaps in periodic fiber reinforced composite materials: the carbon/epoxy composite and some metallic systems.
11. E. N. Economou and M. M. Sigalas 1994 *Journal of Acoustical Society America* **95**, 1735–1740. Stop bands for elastic waves in periodic composite materials.
12. S. Parmley, T. Zobrist, T. Clough, A. Perez-Miller, M. Makela and R. Yu 1995 *Applied Physics Letters* **67**, 777–779. Phononic band structure in a mass chain.
13. M. S. Kushwaha and P. Halevi 1996 *Applied Physics Letters* **69**, 31–33. Giant acoustic stop bands in two-dimensional periodic arrays of liquid cylinders.
14. M. S. Kushwaha and B. Djafari-Rouhani 1996 *Journal of Applied Physics* **80**, 3191–3195. Complete acoustic stop bands for cubic arrays of spherical liquid balloons.
15. M. S. Kushwaha and P. Halevi 1997 *Journal of Acoustical Society of America* **101**, 619–622. Stop bands for cubic arrays of spherical balloons.
16. J. O. Vasseur, B. Djafari-Rouhani, L. Dobrzynski and P. A. Deymier 1997 *Journal of Physics*: *Condensed Matter* **9**, 7327–7341. Acoustic band gaps in fiber composite materials of boron-nitride structure.

17. S. John 1991 *Physics Today* **44**, 32–40. Localization of light.
18. R. L. Weaver 1990 *Wave Motion* **12**, 129–142. Anderson localization of ultrasound.
19. W. A. Smith and B. A. Auld 1991 *IEEE Transactions on Ultrasonics Ferroelectrics, and Frequency Control* **38**, 40–47. Modeling 1–3 composite piezoelectrics: thickness-mode oscillations.
20. W. A. Smith 1992 *Proceedings of SPIE Symposium: New Developments in Ultrasonic Transducers and Transducer Systems* **1733**, 3–26. New opportunities in ultrasonic transducers emerging from innovations in piezoelectric materials.
21. R. Martinez-Sala, J. Sancho, V. Gómez, J. Llinarez and F. Meseguer 1995 *Nature* **378**, 241. Sound attenuation by sculpture.
22. M. M. Sigalas and E. N. Economou 1996 *Europhysics Letters* **36**, 241–245. Attenuation of multiple-scattered sound.
23. M. S. Kushwaha 1997 *Applied Physics Letters* **70**, 3218–3220. Stop bands for periodic metallic rods: sculptures that can filter the noise.
24. M. S. Kushwaha and P. Halevi 1997 *Japanese Journal of Applied Physics* **36**, L1043–L1044. Ultrawideband filter for noise control.